J|A|C|S COMMUNICATIONS

Published on Web 08/26/2010

MRI Detection of VEGFR2 *in Vivo* Using a Low Molecular Weight Peptoid−$(Gd)_8$-Dendron for Targeting

Luis M. De León-Rodríguez,[†] Angelo Lubag,[†] D. Gomika Udugamasooriya,[‡] Bettina Proneth,[‡] Rolf A. Brekken,[‡] Xiankai Sun,[†] Thomas Kodadek,[‡] and A. Dean Sherry*[,†]

Advanced Imaging Research Center, Departments of Internal Medicine, Radiology, Biochemistry and Surgery, University of Texas Southwestern Medical Center, 5323 Harry Hines Boulevard, Dallas, Texas 75390-9185

Received June 24, 2010; E-mail: Dean.Sherry@UTSouthwestern.edu

Abstract: The synthesis of a polylysine dendron containing eight GdDOTA units conjugated to a peptoid dimer known to have a high affinity for the vascular endothelial growth factor receptor 2 (VEGFR2) is described. This simple low molecular weight system with a molecular r_1 relaxivity of ~48 mM^{-1} s^{-1} is shown to enhance MR images of tumors grown in mice *in vivo*.

Magnetic resonance imaging (MRI) is widely used for anatomical imaging of soft body tissues and for measuring dynamic processes such as perfusion, diffusion, and chemical exchange. Paramagnetic complexes (largely Gd^{3+}, Fe^{2+}, Mn^{2+}) are commonly used to enhance contrast differences by altering the inherent relaxation properties (T_1, T_2, T_2*) of tissue water. MR contrast agents are typically given in high doses (0.1 mmol/kg) and consequently are generally considered too insensitive for molecular imaging applications. Consequently, MR contrast agents designed to target specific biostructures are often based on nanoparticle or dendrimer platforms that allow significant amplification by an additive effect of multiple paramagnetic centers over a single center.[1] Although this approach does improve the sensitivity of MR agents, changing from a simple low molecular weight complex to a large particle can have a substantial effect on tissue biodistribution and clearance of the agent. Other factors that can be optimized to decrease the amount of agent needed for detection include increasing its affinity for a target (lowest K_D).[2] We recently demonstrated that a single Gd^{3+}−peptide conjugate targeted to a specific protein attached to agarose beads could be detected by MRI at a local concentration of ~4 μM and, based on those results, predicted that a Gd^{3+}-based agent with a molecular $r_1 \approx 100$ mM^{-1} s^{-1} should be able to detect biological targets present at ~690 nM.[3] However, creating a single low MW agent with an $r_1 \approx 100$ mM^{-1} s^{-1} has proven difficult even with highly motionally restricted systems.[4] A simpler approach would be to attach a few Gd^{3+} chelates each having a more typical r_1 to a targeting moiety such that the molecular r_1 sums to ~100 mM^{-1} s^{-1}. This has been achieved by attaching several Gd^{3+} complexes to a variety of functionalized scaffolds (e.g., polymers, hyperbranched polymers, dendrimers)[5−7] or to nanoparticles,[8] but such large structures can add new complexity by slowing renal filtration rates[9] (glomerular filtration threshold MW ≤ 45 kDa)[5] and even altering biodistribution of the agent. For example, a PAMAM G4 dendrimer with ~21 GdDTPA plus four biotins on its surface for targeting (~29 kD) is retained in the vasculature of a tumor at 24 h simply due to the inherent enhanced permeability and retention (EPR) property characteristic of macromolecules.[10] This feature could make it difficult if not impossible to differentiate a targeted versus a nontargeted macromolecule in tumors. Polylysine-based dendrimers also show promise in that they can be synthesized in specific sizes, they are biocompatible, and their blood clearance rates can be tuned by molecular weight to allow sufficient time to reach their target.[11] Antibodies and peptides have been most widely used for targeting specific biomarkers, but such systems often suffer from poor *in vivo* stability or costly production. More recently, β-peptides and peptoids have gained interest as targeting moieties because they are easy to prepare, cost-effective, and stable toward peptidase and protease activity. Furthermore, screening methods to identify highly specific peptoid targeting agents for specific biomarkers on living cells have been reported.[12] A strategy we have adopted for creating targeted agents for molecular imaging by MRI consists of (1) selection of a target specific moiety from a peptoid library, (2) affinity optimization, (3) attachment of a small poly(GdDOTA)lysine dendrimer scaffold to the targeting peptoid, (4) affinity optimization of the final conjugate, and (5) *in vivo* testing. As an initial demonstration, we utilized a dimeric form of a 9-residue peptoid sequence (GU40C4) known to bind with high affinity to the vascular endothelial growth factor receptor 2 (VEGFR-2),[12] an important target for tumor metastasis. The fluorescein-tagged GU40C4 peptoid displayed a $K_D = 91 \pm 20$ nM for VEGFR-2 (see Supporting Information). A third generation poly(DOTA-lysine) dendron with a lysine linker (Figure 1) was prepared by standard solid phase and solution synthesis followed by addition of a maleimide group to the free α-amino of the linker (Scheme S1, Supporting Information). DOTA was selected as the Gd^{3+} chelate since it forms complexes with high thermodynamic and kinetic stability thus eliminating problems associated with metal release, especially for applications *in vivo*.[13] Dendron conjugation to the GU40C4 peptoid was accomplished by reaction of the thiol group of a Cys residue of the peptoid and the maleimide moiety of the dendron. The r_1 relaxivity of the peptoid−Gd_8-dendron conjugate (**1** in Figure 1) was 13.8 ± 0.2 mM^{-1} s^{-1} (37 °C, pH 7, 23 MHz) per Gd^{3+} ion, slightly higher than the r_1 of the unconjugated Gd_8-dendron (12.3 ± 0.5 mM^{-1} s^{-1}). These r_1 relaxivities are similar to that reported for Gadomer 17 (16.5 mM^{-1} s^{-1} at 25 °C, 20 MHz), a dendritic contrast agent composed of three third generation lysine dendrons attached to a trimesoyl triamide central core.[14] The affinity between conjugate **1** and VEGFR-2, as measured by displacement of the fluorescein-peptoid, was about 7-fold weaker ($K_D = 703 \pm 172$ nM) than unmodified GU40C4, presumably reflecting the steric bulk introduced by the Gd_8-dendron. To test this, a longer linker was introduced between the peptoid and the Gd_8-dendron (**2** in Figure 1). This modification yielded a conjugate with an increased binding affinity ($K_D = 215 \pm 67$ nM) and somewhat higher r_1 (15.1 ± 0.2 mM^{-1} s^{-1}, 37 °C, pH 7, 23 MHz). At 9.4T, the measured r_1 relaxivity of **2** was 6.1 mM^{-1} s^{-1} per Gd at 37 °C so this translates to a molecular relaxivity of ~48 mM^{-1} s^{-1} under the conditions used for *in vivo* imaging. The r_1 value of **2** bound to VEGFR2 on agarose beads did not change significantly so one can reasonably assume that this will be its relaxivity *in vivo* as well.

Porcine aortic endothelial (PAE) and PAE cells expressing human VEGFR2 (PAE/KDR) (2.5×10^5 receptors per cell) were chosen for initial

[†] Advanced Imaging Research Center.
[‡] Departments of Internal Medicine, Radiology, Biochemistry, and Surgery.

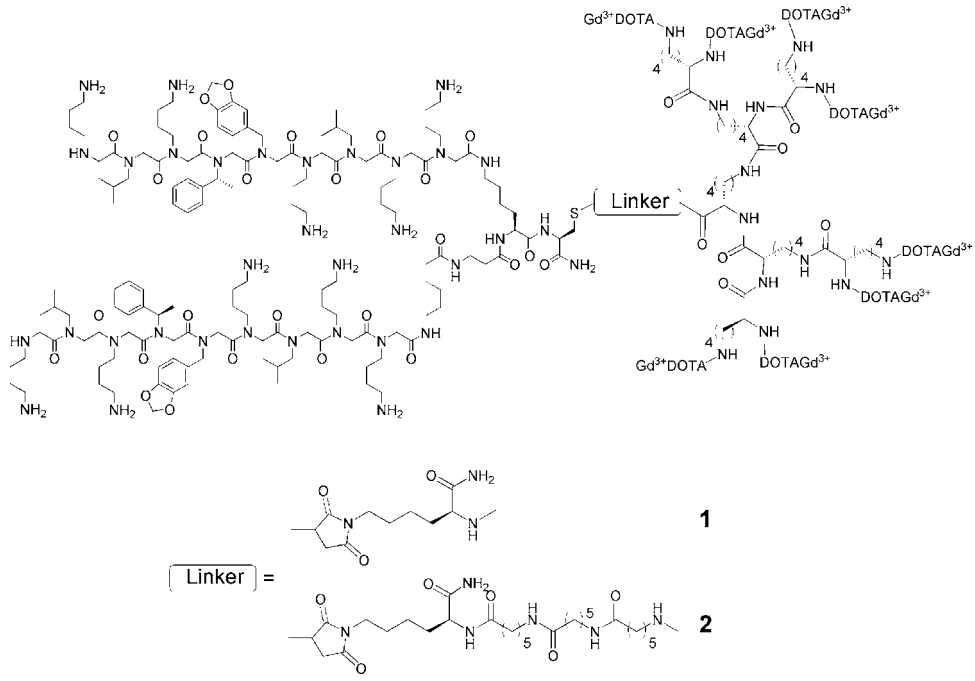

Figure 1. Gd_8-dendron GU40C4 conjugates with different linker chains.

MR imaging. The receptor concentration per cell volume (~5 μm cell radius) was ~790 nM for PAE/KDR while the control PAE cells had no human VEGFR2. Thus, the local concentration of VEGFR2 in PAE/KDR cells was predicted to be within the detection limit for a Gd^{3+} agent having a molecular r_1 of 100 mM^{-1} s^{-1}.[3] T_1 weighted images of both cell lines exposed to **2** or the Gd_8-dendron lacking the peptoid (Figure S4) showed that the image intensity of the PAE cell sample did not change when exposed to either 1.5 μM **2** or the nonconjugated Gd_8-dendron while the PAE/KDR cells showed a significant increase in image contrast only when exposed to **2**, reflecting specific binding of **2** to VEGFR2 on these cells.

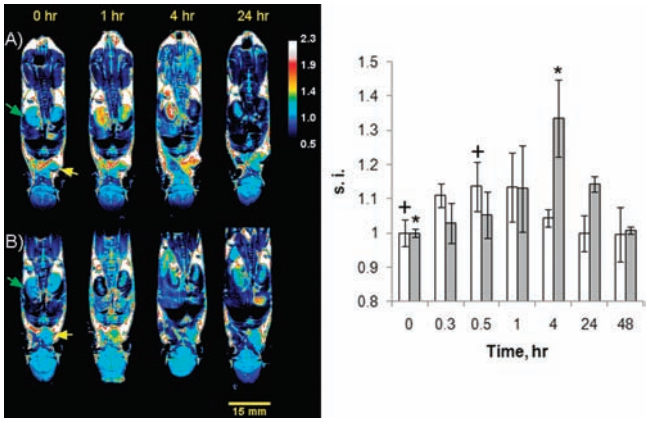

Figure 2. (Left) 9.4 T MR T_1-weighted coronal images of nude mice with subcutaneous cell tumor MDA-MB-231 xenografts at various time points following the intravenous (i.v.) tail injection of Gd_8-dendron peptoid conjugates. (A) images of a tumor-bearing mouse before and after i.v. tail injection of 0.008 mmol/kg of conjugate **2**. (B) Images of another tumor-bearing mouse before and after tail i.v. injection with 0.008 mmol/kg of an indentical Gd_8-dendron conjugated to a control scrambled peptoid. The green and yellow arrows point to a kidney and tumor, respectively. (Right) Tumor signal intensities (s.i.'s) in mice injected with **2** (gray bars) or the control peptoid (white bars) (s.i. is the average of 3 mice) normalized to the tumor intensity prior injection. A t-test (two-tailed, unequal variance) was used to compare s.i. before injection and at 0.5 or 4 h postinjection of the animals injected with the control peptoid (+) or **2** (*) respectively. A $p < 0.05$ was considered statistically significant.

ICP-MS analysis of the cells postimaging showed there was negligible Gd^{3+} associated with either cell line exposed to the nonconjugated Gd_8-dendron while the PAE/KDR cells exposed to **2** had ~900 nM Gd^{3+}. These results show that cell receptors expressed at this level can be detected by MRI using these simple targeted agents.

Next, we moved to an animal model to evaluate whether VEGFR2 expression could be detected *in vivo* using this low MW agent (~8.6 kD). Mice with MDA-MB-231 tumor xenografts known to express VEGFR2[15] were imaged before and after administration of **2** (0.008 mmol/kg). Those results were compared with images of other mice after injection of a scrambled 9-residue peptoid−Gd_8-dendron conjugate (~ 8.4 kD) (0.008 mmol/kg) that does not bind VEGFR2 (Figure S3). As shown in Figure 2 (left panel), tumors in mice treated with **2** were maximally enhanced at ~4 h postinjection (Figure 2A) while the image intensity in tumors after injection of the control peptoid Gd_8-dendron conjugate (Figure 2B) returned to baseline levels by 4 h (Figure 2 right panel). The kidneys of these animals were also monitored during the study. After injection of the control peptoid Gd_8-dendron, the kidneys quickly darkened as a result of a reduction in T_2 as expected during clearance of a Gd^{3+} agent at high imaging fields (Figure 2B).[16] The kidney intensity in animals postinjection of an equivalent dose of **2** did not darken significantly until much later in the study (Figure 2A). This indicates that **2** is largely sequestered elsewhere during these early time points. It has been reported that VEGFR2 is also expressed in other tissues (e.g., kidney, liver) in mice[17] which might explain some of the time dependent contrast differences. The kidney signal intensity in mice treated with **2** and the control peptoid returned to pretreatment levels at 48−72 h postinjection.

In conclusion, we have presented a low molecular weight general targeting platform by combining a peptoid sequence derived from a chemical library with a Gd_8-dendron to generate a high T_1 relaxivity probe for molecular imaging of VEGFR2 *in vivo* by MRI. We anticipate that this platform technology will be generally useful for other targets that exist in tissues at these levels as well.

Acknowledgment. Financial support from the National Institutes of Health (RR02584, CA115531, and CA126608) is gratefully acknowledged.

Supporting Information Available: Calculations, detailed experimental procedures, and characterization data for the compounds discussed in this work. This material is available free of charge via the Internet at http://pubs.acs.org.

References

(1) Villaraza, A. J. L.; Bumb, A.; Brechbiel, M. W. *Chem. Rev.* **2010**, *110*, 2921.
(2) Lee, S.; Xie, J.; Chen, X. *Biochemistry* **2010**, *49*, 1364.
(3) Hanaoka, K.; Lubag, A. J. M.; Castillo-Muzquiz, A.; Kodadek, T.; Sherry, A. D. *Magn. Reson. Imaging* **2008**, *26*, 608.
(4) Kielar, F.; Tei, L.; Terreno, E.; Botta, M. *J. Am. Chem. Soc.* **2010**, *132*, 7836.
(5) Zarabi, B.; Borgman, M. P.; Zhuo, J.; Gullapalli, R.; Ghandehari, H. *Pharm. Res.* **2009**, *26*, 1121.
(6) Swanson, S. D.; Kukowska-Latallo, J. F.; Patri, A. K.; Chen, C.; Ge, S.; Cao, Z.; Kotlyar, A.; East, A. T.; Baker, J. R., Jr. *Int. J. Nanomed.* **2008**, *3*, 201.
(7) Cheng, Z.; Thorek, D. L. J.; Tsourkas, A. *Angew. Chem., Int. Ed.* **2010**, *49*, 346.
(8) Warsi, M. F.; Adams, R. W.; Duckett, S. B.; Chechik, V. *Chem. Commun.* **2010**, *46*, 451.
(9) Ye, F.; Jeong, E. K.; Jia, Z.; Yang, T.; Parker, D.; Lu, Z. R. *Bioconjugate Chem.* **2008**, *19*, 2300.
(10) Zhu, W.; Okollie, B.; Bhujwalla, Z. M.; Artemov, D. *Magn. Reson. Med.* **2008**, *59*, 679.
(11) Langereis, S.; Dirksen, A.; Hackeng, T. M.; Van Genderen, M. H. P.; Meijer, E. W. *New J. Chem.* **2007**, *31*, 1152.
(12) Udugamasooriya, D. G.; Dineen, S. P.; Brekken, R. A.; Kodadek, T. *J. Am. Chem. Soc.* **2008**, *130*, 5744.
(13) Cabella, C.; Crich, S. G.; Corpillo, D.; Barge, A.; Ghirelli, C.; Bruno, E.; Lorusso, V.; Uggeri, F.; Aime, S. *Contrast Media Mol. Imaging* **2006**, *1*, 23.
(14) Nicolle, G. M.; Tóth, E.; Schmitt-Willich, H.; Radüchel, B.; Merbach, A. E. *Chem.—Eur. J.* **2002**, *8*, 1040.
(15) Roland, C. L.; Dineen, S. P.; Lynn, K. D.; Sullivan, L. A.; Dellinger, M. T.; Sadegh, L.; Sullivan, J. P.; Shames, D. S.; Brekken, R. A. *Mol. Cancer Ther.* **2009**, *8*, 1761.
(16) Caravan, P.; Farrar, C. T.; Frullano, L.; Uppal, R. *Contrast Media Mol. Imaging* **2009**, *4*, 89.
(17) Maharaj, A. S. R.; Saint-Geniez, M.; Maldonado, A. E.; D'Amore, P. A. *Am. J. Pathol.* **2006**, *168*, 639.

JA105563A